Rolling contact fatigue in relation to rail grinding

Steenbergen, Michaël

DOI
10.1016/j.wear.2016.03.015

Publication date
2016

Document Version
Accepted author manuscript

Published in
Wear

Citation (APA)
Steenbergen, M. (2016). Rolling contact fatigue in relation to rail grinding. *Wear*, *356-357*, 110-121.
https://doi.org/10.1016/j.wear.2016.03.015

Rolling Contact Fatigue in relation to rail grinding

Michaël Steenbergen*

Delft University of Technology, Faculty of Civil Engineering and Geosciences, Railway Engineering Group, Stevinweg 1, 2628 CN Delft, the Netherlands

---

Abstract Spalling defects of a periodic nature are sometimes observed on heat-treated pearlitic steel rails. Defect properties suggest that there may be a relationship between maintenance grinding on a regular basis and the initiation of rolling contact fatigue (RCF). In this work, the effects of maintenance grinding are investigated experimentally for both standard and heat-treated pearlitic rails. Results show essentially different behaviour for both steels. On standard grades, friction-induced martensite (FIM) generated during grinding delaminates when in service. However, grinding induces severe top-layer deformation which coincides with that induced by train operation, thus yielding 'pre-fatigue' of the rail. On heat-treated grades, portions of FIM accumulated at groove edges during grinding are pressed into the deeper pearlitic matrix in combination with severe plastic deformation under tangential wheel-rail contact stresses. That process results in severe and extensive crack initiation. According to quantitative test results reported in the literature, this initial condition yields a reduction of the normal RCF life by roughly a factor nine, which is in accordance with both observations in the field and in the literature on rail spalling defects.

Keywords: Rail grinding, white etching layer (WEL), rolling contact fatigue (RCF), friction-induced martensite (FIM), squat, rail spalling, residual stress.

1. Introduction

Recently, an increase in the number of particular rail spalling defects has been noticed on the Dutch rail network. The defects occur typically on heat-treated grades such as MHH (produced by Tata and belonging to the category R370crHT according to the European norm [1]). At first glance, it seems to concern a hybrid defect type with properties of both short-pitch corrugation and rolling contact fatigue (RCF). The defects are characterised by their affected length (with in some cases up to several hundreds of meters of affected rail), by the periodicity in the geometry of the defect, and

* Corresponding author. Tel. +31 15 2783385; fax: +31 15 2783443
E-mail address: M.J.M.M.Steenbergen@tudelft.nl (M.J.M.M. Steenbergen)

by the fact that the cracks associated with the defects propagate systematically in the subsurface and do not develop deep into the railhead, leading to transverse defects. Examples are shown in Fig. 1.

Fig. 1   Periodic spalling defects on heat-treated rail grade R370crHT/MHH

On other rail networks, individual spalling defects with similar properties and behaviour have been noticed and called ‘studs’, a term introduced by Grassie [2] in order to differentiate them from squat defects. ‘Studs’ were observed to grow relatively much faster than squats and at the same time did not lead to transverse defects [3].

All affected rails perform in the RCF regime (in contrast to the wear regime [4]) and are therefore maintained by cyclic grinding. The defects develop relatively very early in the maintenance cycle of the rail, within the grinding interval of 15 megatons of axle loading; however not necessarily on relatively new rail but also on rail that has already been in service for years. Properties of the rail defects will be addressed in more detail and in a wider context in the next section. Several of these properties however are striking, and together with the early development of the defects in the maintenance cycle, they point into the direction of a potential role of the grinding process with respect to damage initiation. This leads to a more general research question: how does rail maintenance grinding (or: the set of operational specifications that control this process) affect the total life cycle of the rail – is rail grinding purely a solution to combat RCF, or has grinding the potential to determine the further degradation of the rail surface by setting the conditions for the further development of RCF? The aim of this paper is to examine the role of the rail grinding process, as it is practised on the Dutch network and many other networks worldwide, with respect to RCF initiation, differentiating between heat-treated and conventional rail grades. Its main novelty consists of an answer to this question, substantiated by experimental results. Because of the number of involved aspects and parameters, such as the speed and other settings of the grinding equipment/train, which determine the specific energy input per surface area unit, and the exact chemical composition and constitutive properties of different rail grades, this first study is at the same time of a preliminary nature. It is limited to two pearlitic rail categories specified in the European norm [1], one standard carbon grade (R260Mn) and one heat-treated and alloyed grade (R370crHT, in the form MHH produced by Tata).

The paper focusses explicitly on the 'initial conditions' of the rail surface degradation process as a function of borne tonnage, and not on this degradation process itself and its governing parameters, as these initial conditions may have an influence that may in theory even exceed that of the loading history on the final result in terms of damage. It is further common experience that the degradation process on rails on which not all surface damage, in terms of RCF cracks, has been removed to a sufficient depth (an example is shown in Fig. 2), is only briefly slowed down by the grinding process. In fact, the geometrical irregularity associated to the RCF defect has been removed, but as this irregularity is only a consequence and not the origin of the defect, the presence of surface-breaking cracks continues to affect the local wheel-rail contact stress distribution and therefore the defect continues to grow. This particular aspect of rail grinding is however not within the scope of this paper, which addresses the grinding process (and indirectly its operational specifications) as such.

Fig. 2   A squat ground to an insufficient depth

The formulated research question has received some direct and indirect attention in the scientific literature, but both the research approach and the results are insufficient to answer it adequately. The most relevant work in the literature is a study by Dikshit et al. [5]. This work examined, in the framework of early RCF, samples of heat-treated rail at different moments of the life cycle of the rail, which was ground also upon installation. The analysis included the moment directly prior to maintenance grinding and a moment at 1 MGT after grinding. It was shown that the number of small (smaller than 0.1 mm) cracks was greatest very early in the life of the rail and steadily decreased with born tonnage up to maintenance grinding, whereas the number of long cracks consistently increased. Significant parts of the rail surface were found to be covered with a white etching layer (WEL) at lower tonnage and formed very early in the rail life, decreasing – by a mechanism of spalling wear – with increasing tonnage. However, as the study does not include analyses of the surface conditions shortly after rail grinding but only after 1 MGT of loading, a potential role of the grinding process with respect to the both the generation of WEL and crack initiations was disregarded; their arising early in the rail life was speculatively ascribed to wheel-rail contact conditions. A second study [6] addresse the effect of rail grinding on RCF on standard rail in the Japanese network. This study however deals with the depth to be removed in order to erase all plasticity as a result of accumulated tonnage and does not address the surface quality. Apart from these studies specifically in the rail context, more general work has been reported in the literature on the relationship between surface finishing methods and RCF life [7-10]. These studies will be discussed in more detail, in the framework of a validation of the outcome of the present work, in section 5.

The structure of the rest of this paper is as follows. Section 2 continues with a more detailed investigation of the properties of the observed spalling defects in the framework of other damage types and of grinding results; section 3 discusses the set-up of a field experiment with respect to rail grinding; section 4 presents and discusses experimental results; section 5 discusses these results in the framework of other/recent scientific work and developments, and section 6 finishes with conclusions.

2. Properties of rail spalling defects versus rail grinding results

Fig. 3 shows images of rails after cyclic (rotational) grinding with a grinding train and a relatively short period of short train loading afterwards. In both cases the grinding facets have worn out; in the case at the left a repetitive groove pattern is visible, whereas in the case at the right a clear short-pitch, wavy pattern in the running band has developed. The periodicity typically ranges from 34 to 38 mm.

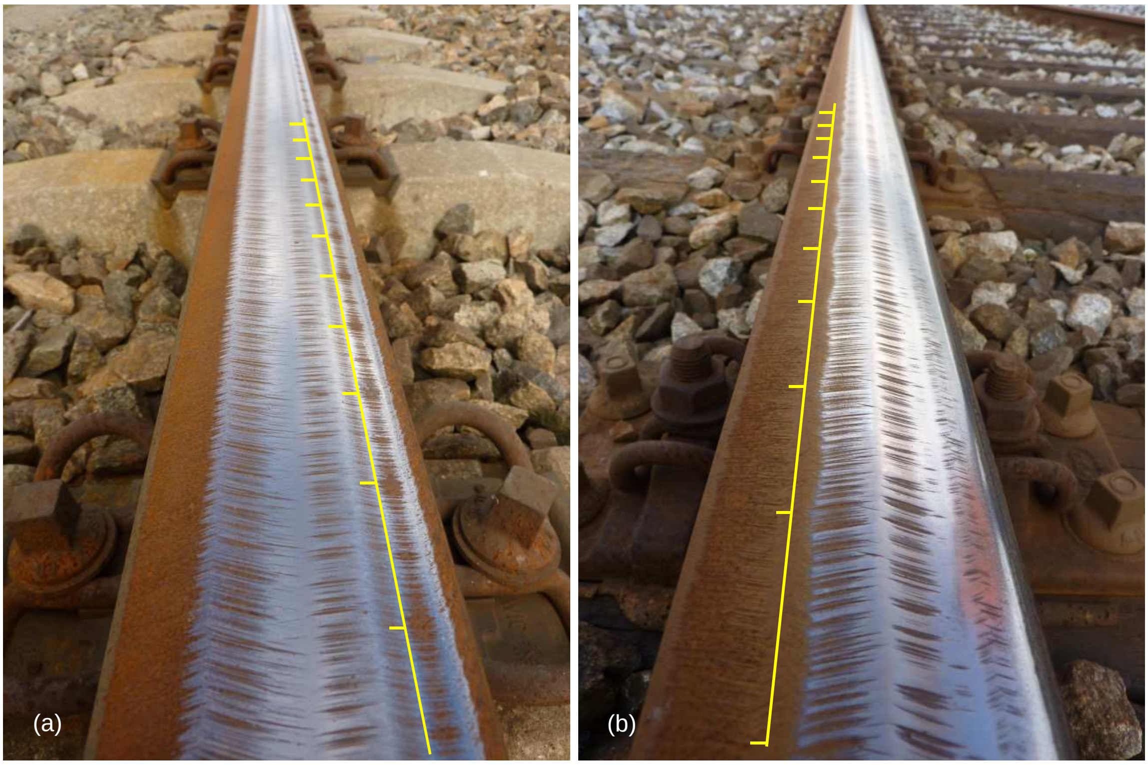

Fig. 3 Rail after grinding and a relatively small born tonnage: longitudinal grinding facets have disappeared – transverse grooves are still present; (a) periodicity and (b) waviness of the running band.

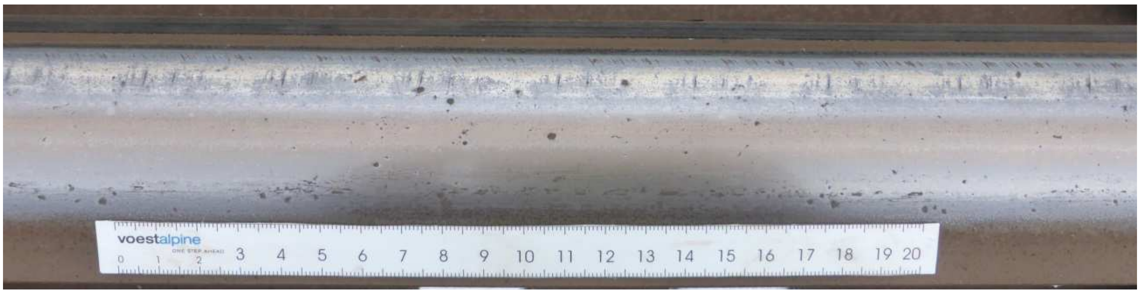

Fig. 4 Periodicity (about 34 mm) in both WEL and grinding marks at the gauge corner of a R260Mn rail (upper leg of a curve)

Fig. 4 shows a situation in the high leg of a curve with contact concentrating on the gauge corner, where a non-uniform white etching layer (WEL) pattern has developed at the surface with a periodicity (34 mm) coinciding with that of the grinding pattern. Fig. 5 shows examples of standard rails (grade R260Mn) where a non-uniform WEL pattern is visible at the surface, in this case with a 36 mm periodicity and WEL-zones in the form of 'eggs' embedded in the running band. Fig. 6 shows the longitudinal surface hardness pattern of such a rail, along with some microstructural features: the hardness clearly fluctuates periodically with extreme values at the centre of the egg-shaped WEL zones and minima, with the original hardness, in between. Fig. 7 shows again a well-developed periodic (36.5 mm) WEL formation in the running band, in this case already associated with short-pitch corrugation, though only with an amplitude in the order of 10 μm. Fig. 8 shows the periodicity in the spalling defect (with individual defects resembling squats), as discussed in the introduction (Fig. 1), with again the typical distance of 35 mm. Finally, Fig. 9 shows a developing long spalling defect where the relationship to the grinding effects is particularly evident: cracks have initiated along the periodic zone with the deepest grinding marks and grown together; surface etching clearly shows that the grinding marks are bordered by white etching material. Also in the case of unbranched squats cases occur where the same periodicity can be observed; an example is given in ref. [11] (Fig. 17 from this work; periodicity 34 mm); Fig. 9 shows another example from the high leg of a 1500 m radius curve.

Fig. 5 Periodicity (35-36 mm; half the rail width of 70 mm) in WEL (‘egg’-shaped) in the running band of R260Mn rail

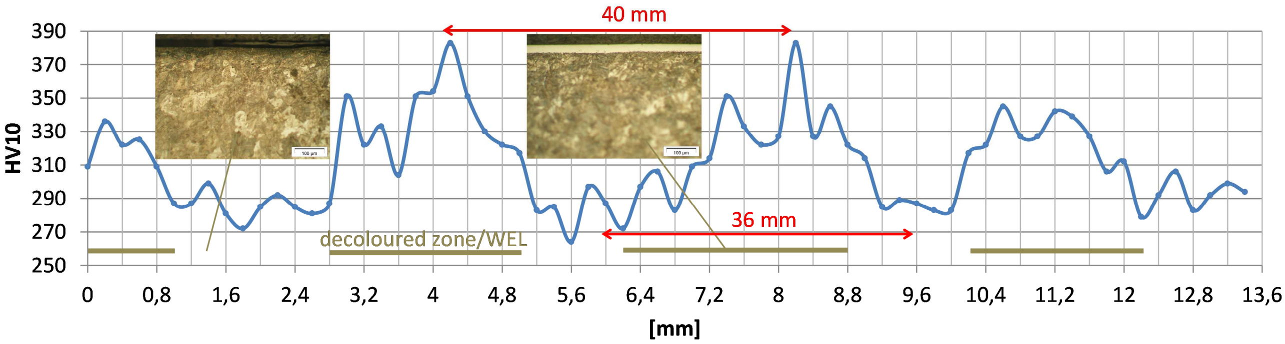

Fig. 6 Longitudinal hardness profile along a R260Mn grade rail with periodicity in material properties/WEL (thickness roughly 30 µm) due to contact stress periodicity

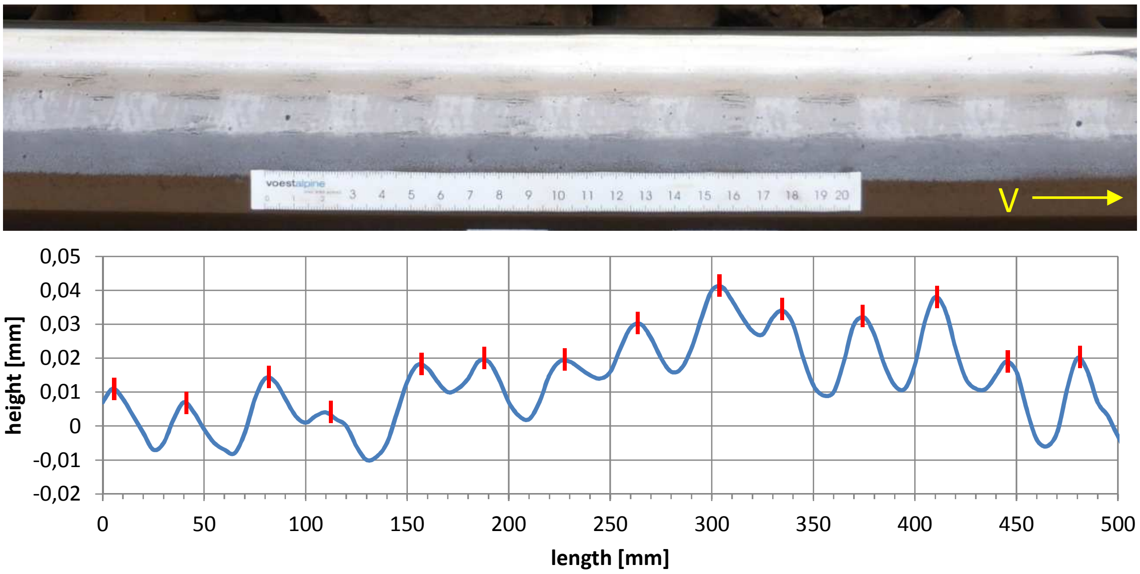

Fig. 7 Periodicity (36,5 mm average) in both WEL (top) and the height of associated short-pitch corrugation (bottom) in the running band of R260Mn rail

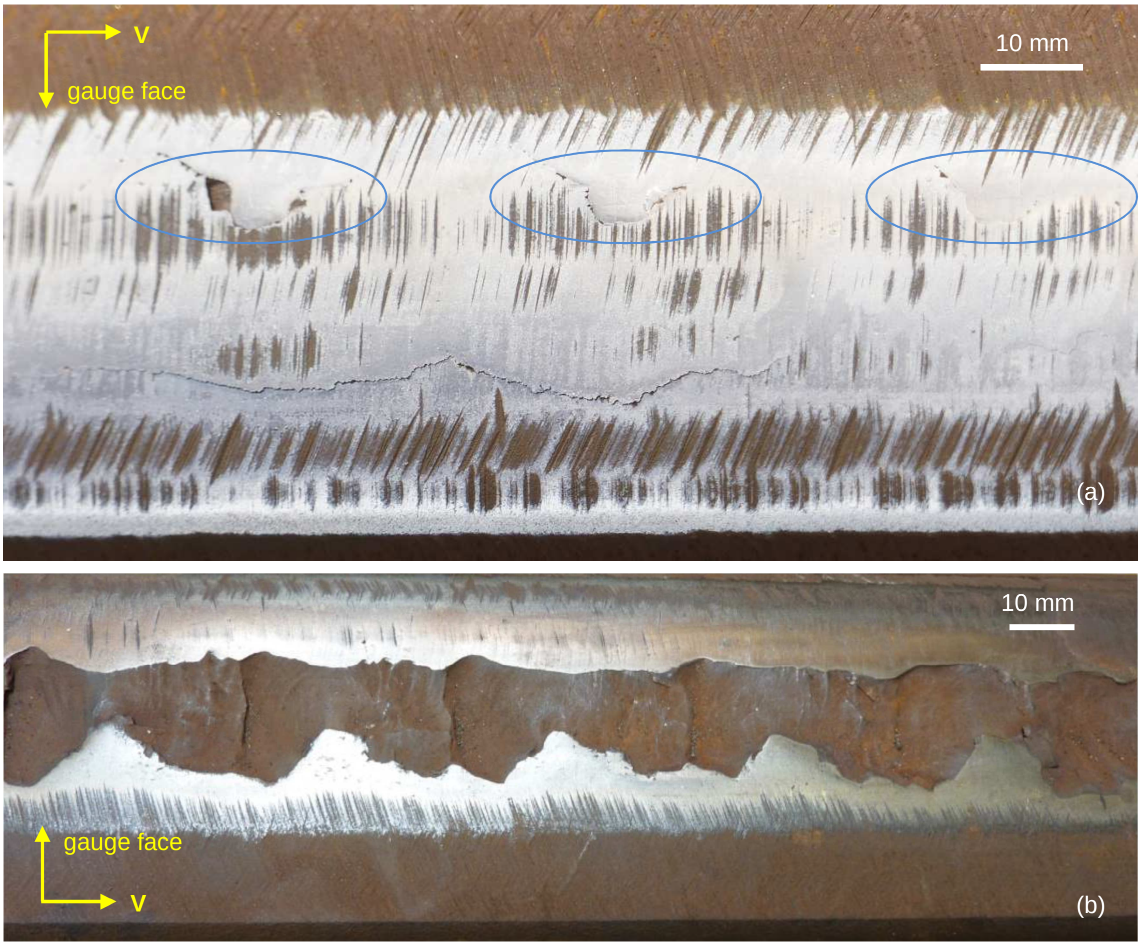

Fig. 8 Periodic (about 35 mm) spalling defects (as in Fig. 1), before (a) and after (b) spalling off, in the running band of two R370crHT/MHH rails

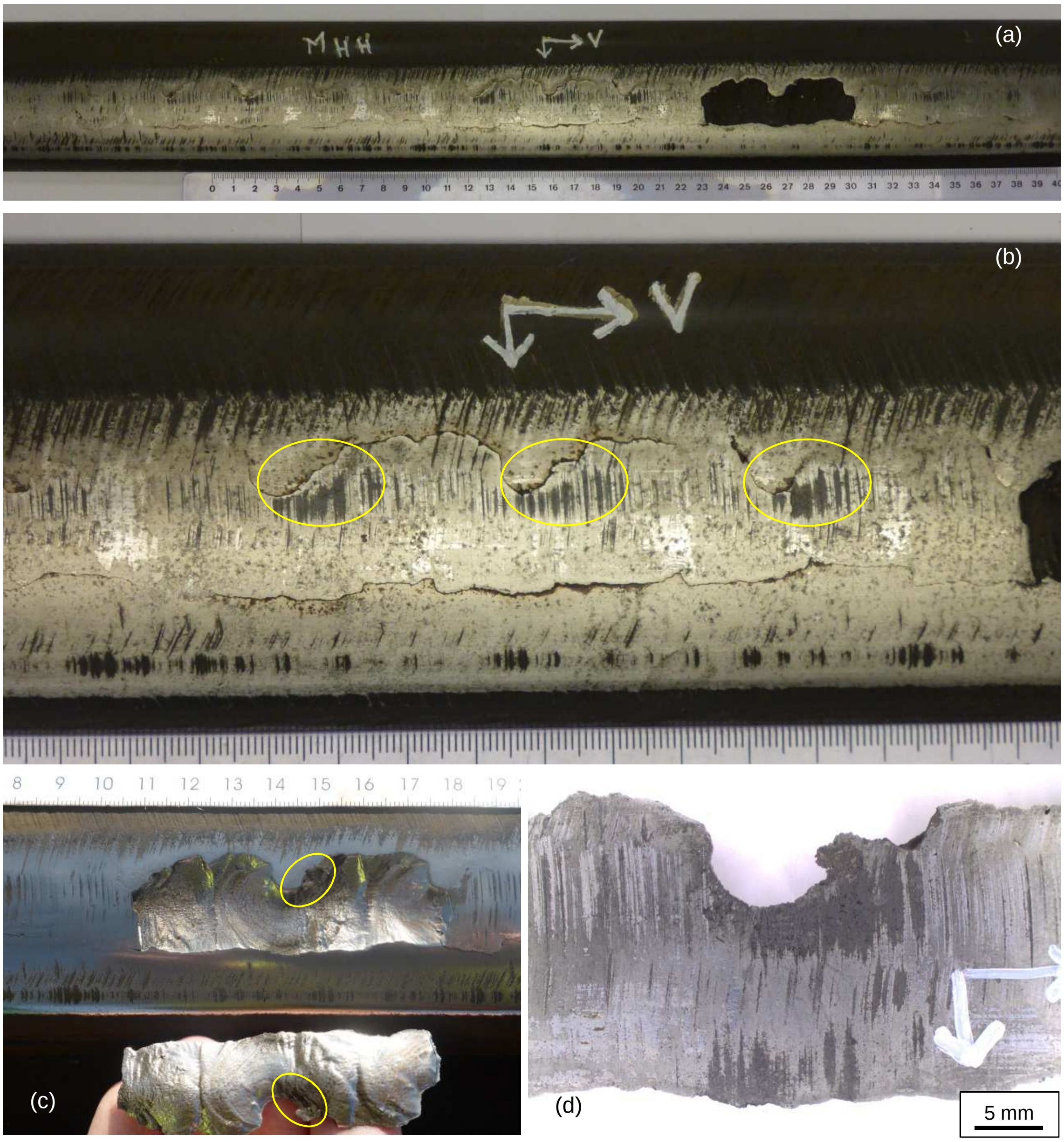

Fig. 9 Periodic spalling defect on ground R370crHT/MHH rail (a): crack initiations along the periodic zones with deepest grinding marks (b, c) and FIM visible on the surface (etched with 5 percent Nital) of the spalled part along the grinding marks (d).

The findings presented in this section show a coincidence between different forms of periodicity: a geometrical one induced by train grinding, one in constitutive material behaviour (WEL formation) and properties in the running band, and one in the development of RCF cracks and eventually spalling defects. From a theoretical viewpoint, geometrical periodicity induces fluctuating normal but notably also tangential contact stress conditions, which may lead to non-uniform shakedown of the rail surface material, non-uniform slip and WEL generation, and finally to periodic RCF initiation and spalling defects. Although the formation of WEL as well as crack initiation seemed in some cases in practice clearly related to the grinding results, this yields in itself no conclusive evidence that grinding effects may induce crack initiation. In order to clarify unequivocally the role of maintenance grinding of the rail in relation to eventual early damage development, the more general research question discussed in the introduction was formulated and an experimental programme was conducted.

3. Experimental set-up

Grinding is supposed to ‘reset the initial conditions’ of the rail life. Therefore, the aim of the experimental programme was to establish these conditions for the treated surface of both standard carbon (R260Mn) and heat-treated pearlitic rail grades (R370crHT/MHH). For both grades, a regular track was selected in the Dutch network with mixed passenger and freight traffic, where cyclic maintenance grinding (with a nominal take-off of 0.2 mm) was to be performed by the grinding train (Speno RR64M with flat rotational grinding principle). The R260Mn sample was taken from straight track and the R370crHT/MHH sample from the high leg of a curve. A rail sample of 75 mm length was taken out immediately after the grinding train had passed and replaced by an enclosed arc welding. This was repeated after a few days of train operation and thus a relatively very small number of train passages. This setting was chosen to investigate the effect of a combination of normal and tangential stresses on the freshly ground surface for a limited number of wheels, at the offset of the loading history; this loading history itself as well as an eventual difference in the loading parameters as a result of track configuration were of minor importance. In this way, four rail samples were collected in total. Figs. 10 and 12 show the two samples collected for each of the grades R260Mn and R370crHT/MHH respectively; Fig. 11 shows a close-up of the ground surface in Fig. 10.

For each of the four samples, both transverse and longitudinal cross-sections were examined with etched microscopy. Longitudinal cross-sections were taken out along the centre of a grinding facet, globally at the centre of the running band, and at the same transverse position both immediately after grinding and after a few days of train operation. Transverse cross-sections covered all transitions between grinding facets.

Fig. 10 Surface of heat-treated rail (R370crHT/MHH) immediately after grinding (right) and a few days of train operation (left); examined longitudinal and transverse cross-sections.

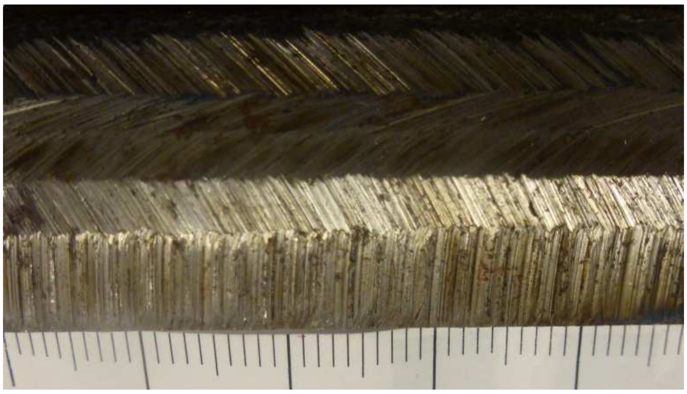

Fig. 11 Close-up of Fig. 10: heat-treated rail (gauge corner) surface roughness and facets immediately after grinding.

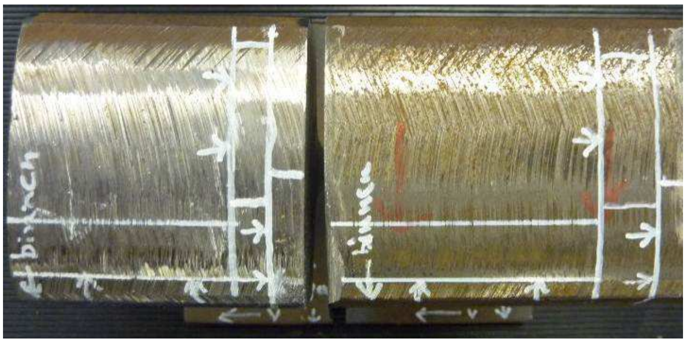

Fig. 12 Surface of standard carbon rail (R260Mn) directly after grinding (left) and a few days of train operation (right); examined cross-sections along the surface.

4. Results of microstructural analysis

Before addressing the results, some basics on the formation of white etching surface material on the rail are briefly recapitulated; a more detailed review of the literature in this domain can be found in earlier work [12]. There are essentially two mechanisms that lead to the formation of a hard and brittle white etching surface layer: the first one occurs due to storage of potential (or strain) energy in the material; the second due to addition of thermal energy. In the first case, an ongoing loading process with notably tangential wheel-rail contact stresses and a ratchetting strain response leads to dissolution of cementite in the pearlitic matrix at the surface and the formation of an amorphous nano-sized structure with a hardness exceeding that of the parent material with a factor 2 to 4. The layer, although it has geometrically clearly determined properties in a cross-section over the height, typically has a more gradual transition to the parent material in the sense of varying grain size and orientation, and also the properties within the layer itself are a function of depth. In the second case, the input of heat at the contact may cause the surface material to reach the austenitization temperature, yielding a phase transition to martensite. Visually and in microscopic research, the effect is very similar to the first case, with a distinct white surface layer with increased hardness, but this layer has a discrete transition to the parent material having a different phase; its properties are constant over the height of the layer and in many cases internal grain boundaries remain visible. This second type of white etching layer is also denoted as FIM (friction-induced martensite). There exist also hybrid layer types, as the presence of plastic strain energy in the material lowers the austenitisation temperature, and in practice such hybrid layers prevail.

Fig. 13 shows different surface positions of a transverse cross-section of standard carbon rail (R260Mn) immediately after grinding. Observations of this cross-section show clearly the transitions between grinding facets, further the presence of a phase-transformed white etching FIM layer, deposits of which typically accumulate at the borders of the grinding facets, and finally a plastic deformation of the top layer which is strongly facet-dependent, and therefore non-uniform over the railhead. This deformation is however directed towards the inside of the rail on the part of the profile bordering the gauge corner. Longitudinal cross-sections (Fig. 14) show grinding grooves, non-uniform loose portions of FIM, and the absence of severe longitudinal plastic deformation texture along the rail surface.

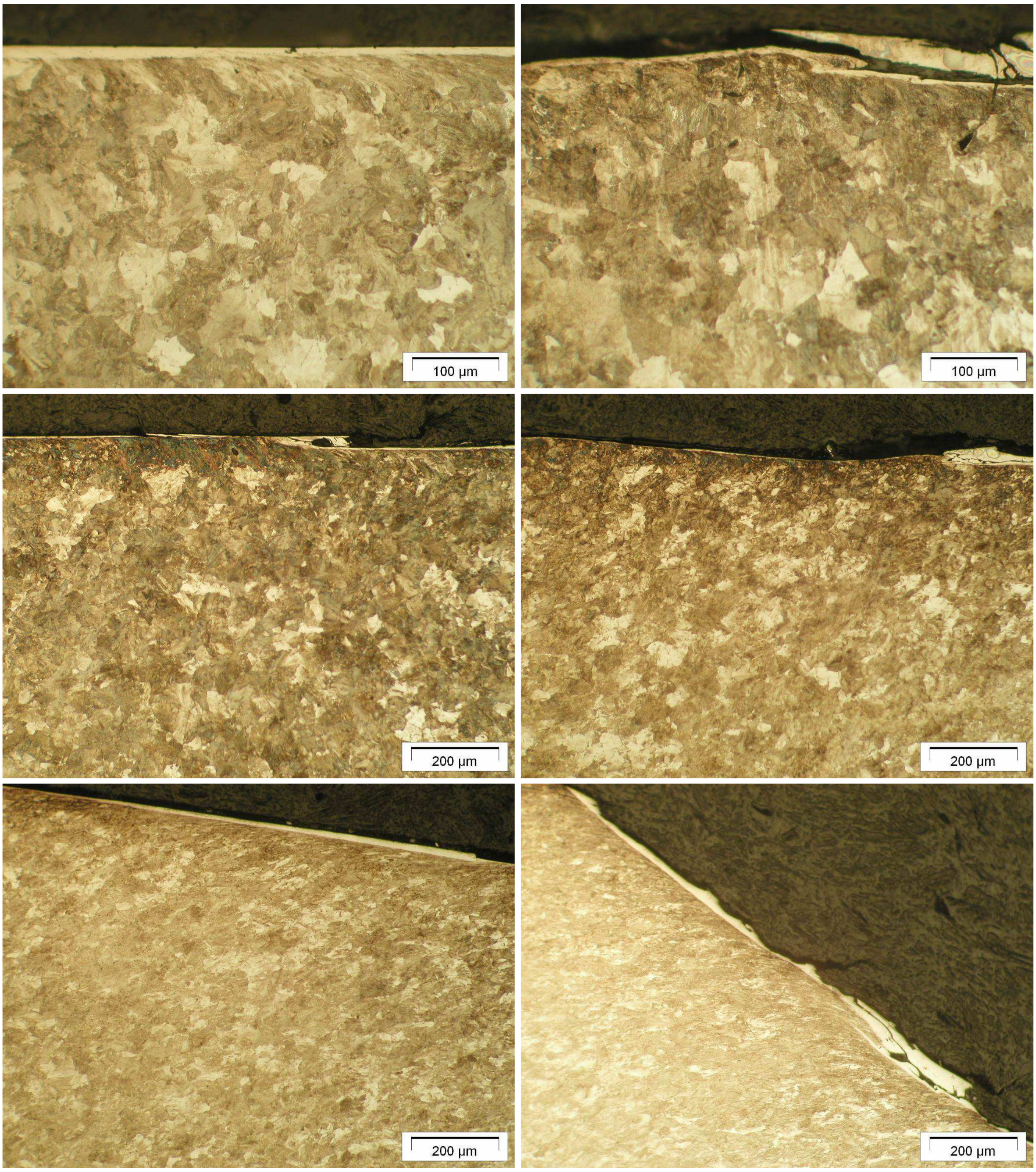

Fig. 13 Surface (transverse cross-section) of standard pearlitic rail (R260Mn) *immediately* after grinding: FIM and strongly facet-dependent plasticity. Images are taken from the field to the gauge side (at the right).

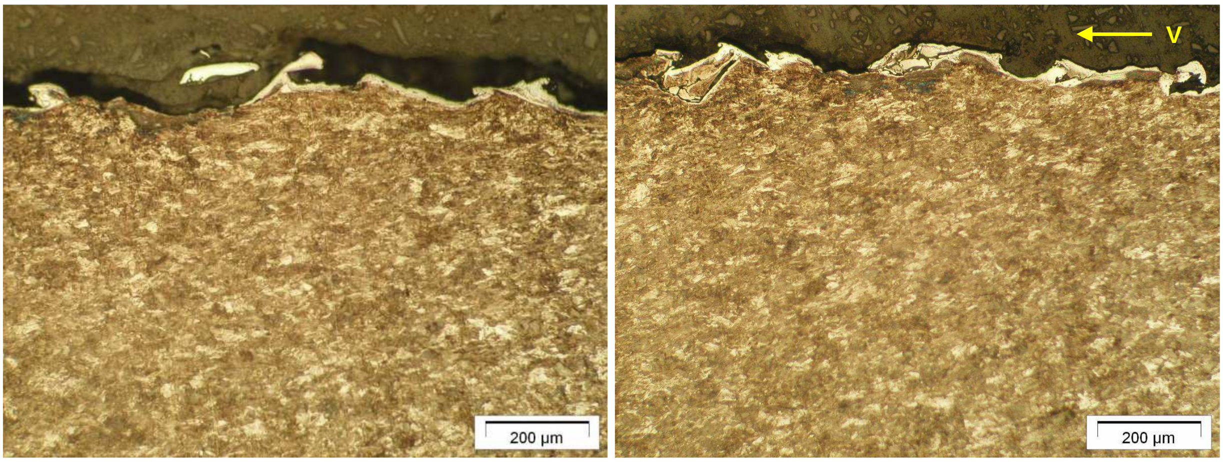

Fig. 14 Surface (longitudinal cross-section) of standard pearlitic rail (R260Mn) *immediately* after grinding: FIM and negligible plasticity. The train running direction is to the left.

Fig. 15 shows the longitudinal rail surface after rail grinding and a few days of train operation consecutively: the FIM generated by grinding is largely removed; individual grooves have disappeared, and severe plastic strain of the pearlite matrix under the surface has appeared as a result of tangential forces by train operation. In transverse direction, also transitions between grinding facets have disappeared.

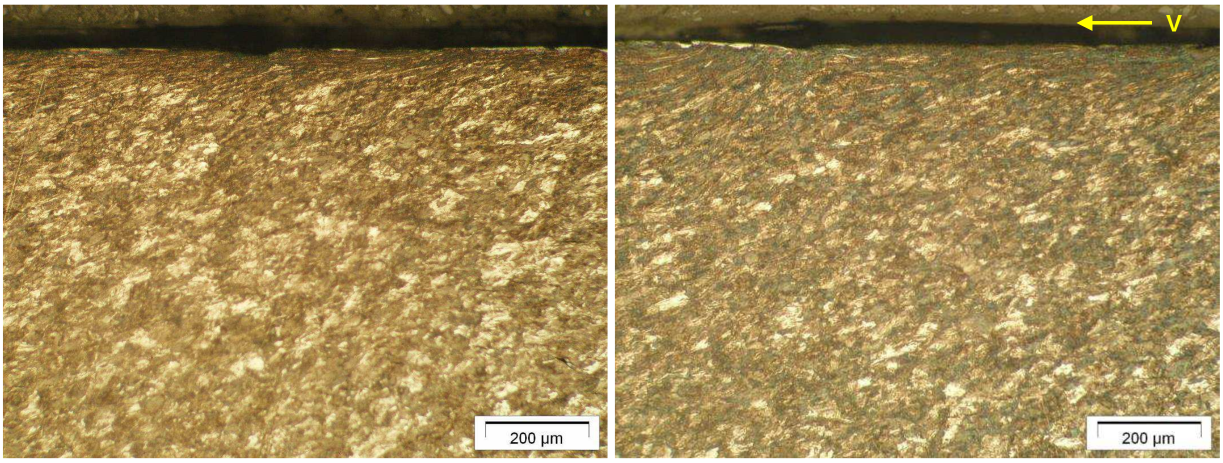

Fig. 15 Surface (longitudinal cross-section) of standard pearlitic rail (R260Mn) *after grinding and a few days of train operation consecutively*: FIM is largely removed; severe train-induced plastic strain has appeared.

Results on heat-treated premium rails (R370crHT/MHH) are essentially different from that on standard rails. Fig. 16 shows different surface positions of the transverse cross-section immediately after grinding. Thick FIM layers are present at many positions; remarkable is their stratification, which causes many of them to delaminate; FIM is present at the surface over the whole cross-section Further, a strongly facet-dependent plastic deformation of the surface layer is present, directed toward the inside on the gauge half of the rail and the outside on the field half of the rail crown.

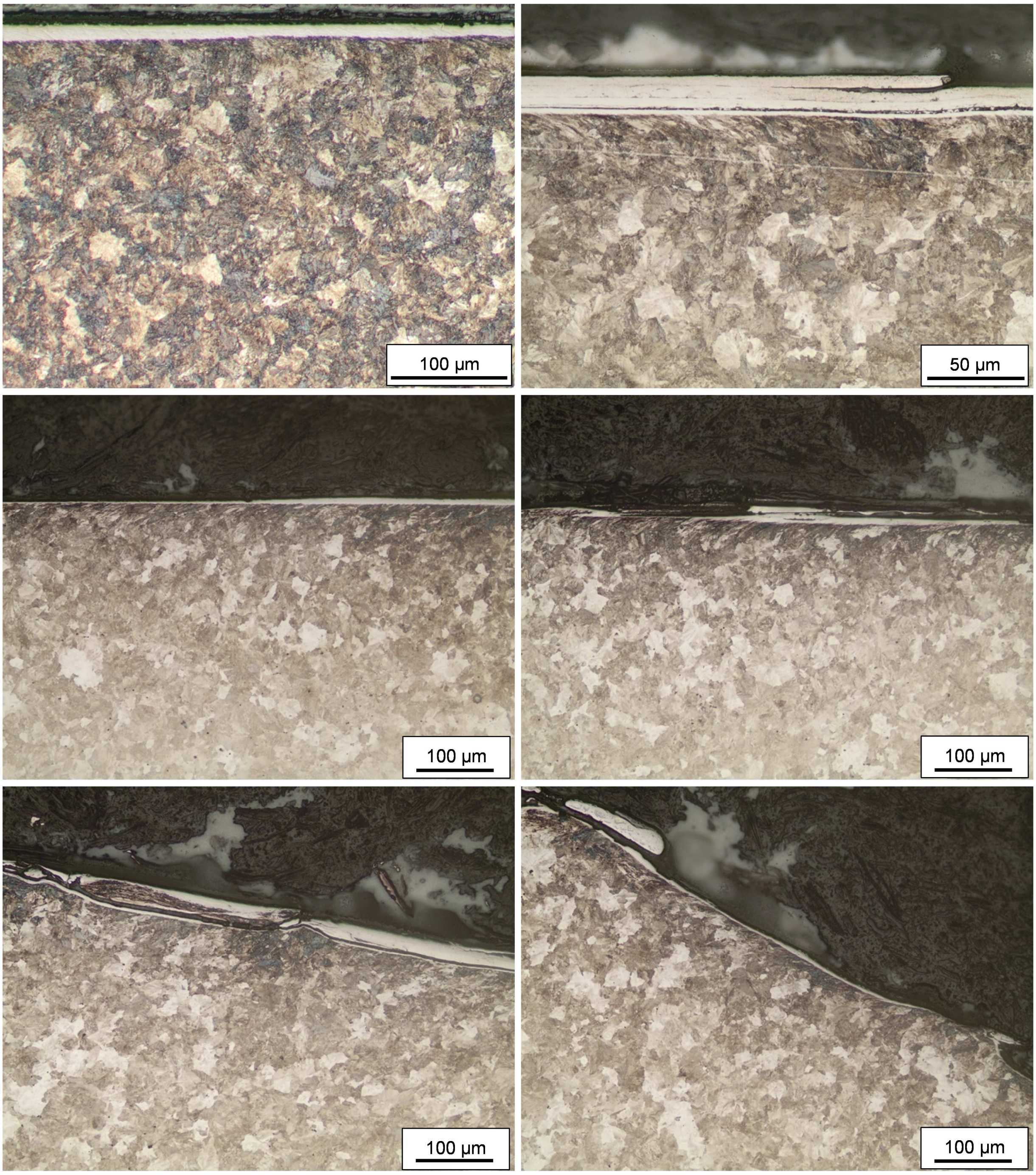

Fig. 16 Surface (transverse cross-section) of heat-treated pearlitic rail (MHH) *immediately* after grinding: FIM layers and strongly facet-dependent plasticity. Pictures are taken from the field to the gauge side (at the right).

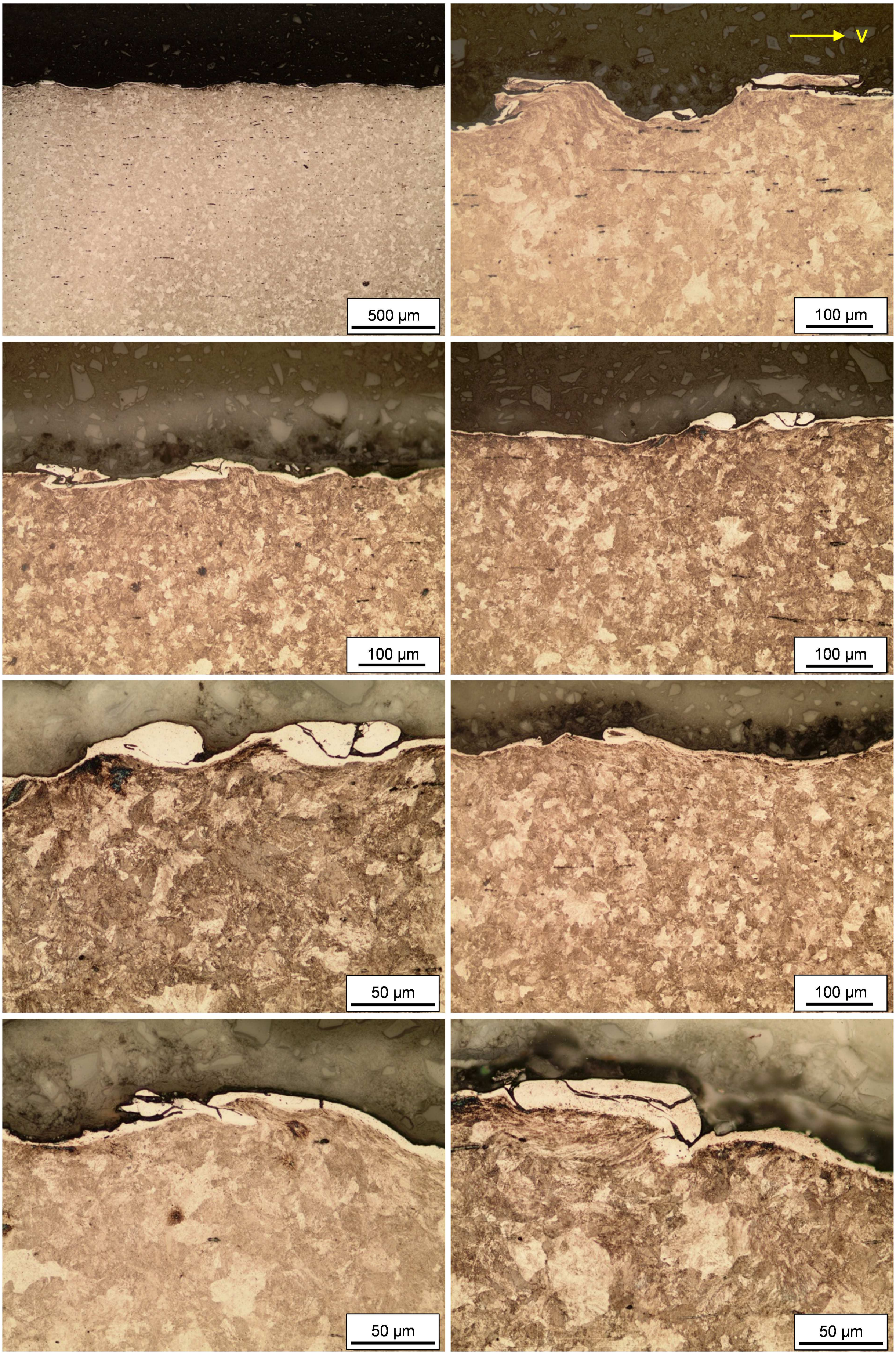

Fig. 17 Surface (longitudinal cross-section) of heat-treated pearlitic rail (MHH) *immediately* after grinding: FIM deposits and localised severe plastic strain.

Positions along the longitudinal cross-section (Fig. 17) show grinding grooves with severe localised plastic deformation and large portions of FIM, typically in the form of deposits at the edges of the grooves. Further, no uniform longitudinal plastic deformation texture of the top layer along the rail surface can be observed.

Fig. 18 shows the longitudinal rail surface after rail grinding and a few days of train operation consecutively: large amounts of FIM generated by grinding are largely removed by spalling wear; there is no uniform plastic deformation along the surface as a consequence of wheel-rail contact. However, at the same time individual portions of FIM are pressed into the surface, along with strong localised plastic strain under tangential stresses exerted in the wheel-rail contact patch. This phenomenon leads to local failure of the granular matrix and crack initiation: the surface is strewn with initiations up to depths of tens of micrometres, with subsurface crack paths propagating against the train running direction. Apparently, the work hardening capacity of the heat-treated material is not sufficient to accommodate the ‘imprint’ of the hard FIM portions in an elastic mode. The density of the crack initiations is correlated with the surface roughness (Fig. 11): each major FIM deposit at the edge of a major groove is a potential crack initiator. In the present case, crack initiations are – very roughly – interspaced at 1 mm. In the transverse direction (not shown), no significant developments can be observed with respect to the situation immediately after grinding; although many stratified FIM layers have delaminated and disappeared, the surface is still largely covered with a single FIM layer; transitions between grinding facets have not changed during the duration of the experiment. It is noted finally that the results of the microstructural analysis coincide with the conclusion from the non-destructive research discussed in section 2, where at the surface of R370crHT/MHH grinding grooves were found to be bordered by FIM (Fig. 9).

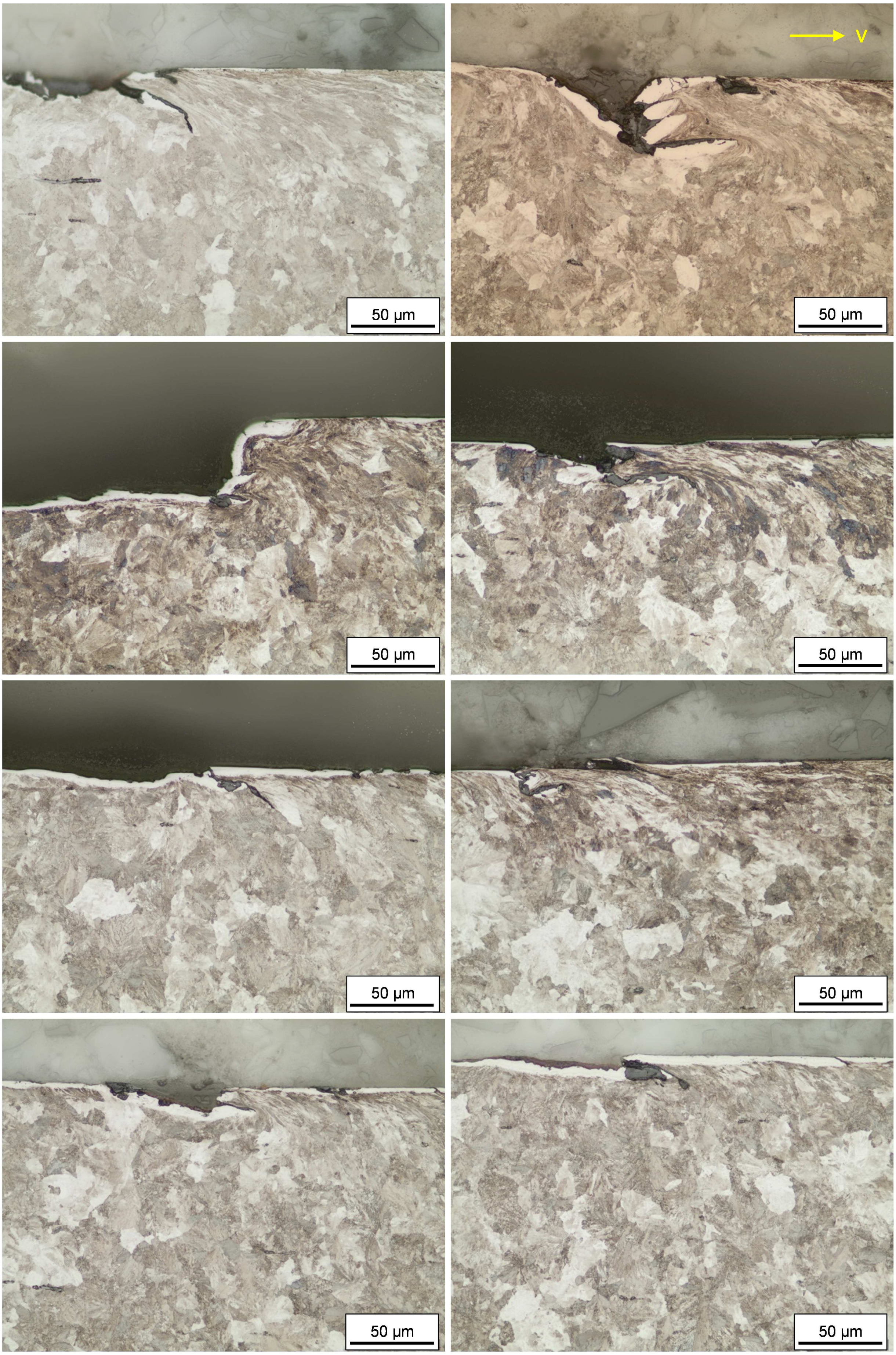

Fig. 18 Surface (longitudinal cross-section) of heat-treated pearlitic rail (MHH) *after grinding and a few days of train operation*: FIM and train-induced plastic strain cause severe crack initiation.

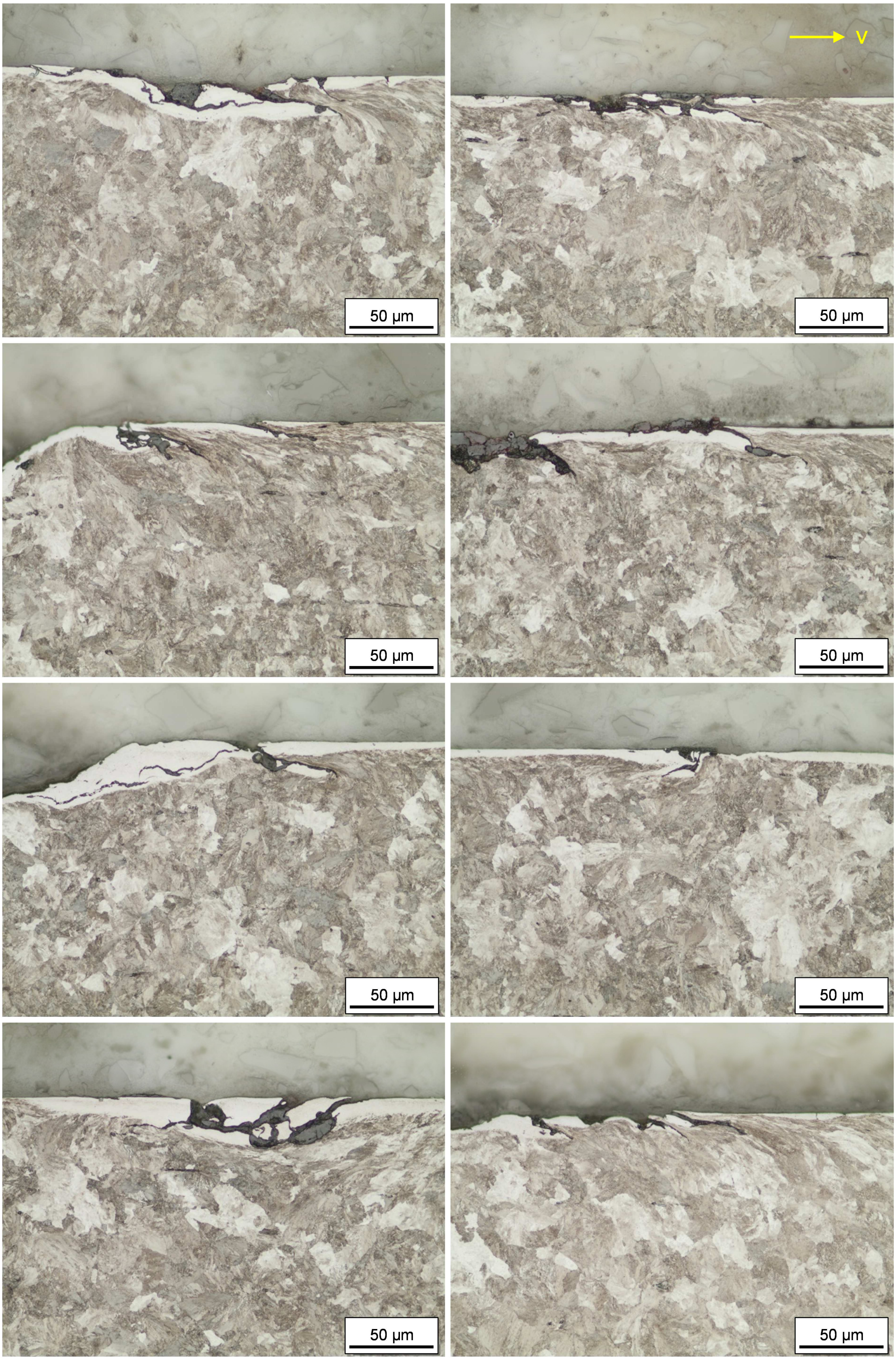

Fig. 18 (continued) Surface (longitudinal cross-section) of heat-treated pearlitic rail (MHH) *after grinding and a few days of train operation*: FIM and train-induced plastic strain cause severe crack initiation.

5. Discussion

Although the experimental results do not clarify the growth of running band defects related to grinding in all its aspects, they clearly provide a differentiated answer to the research question: according to current practice and operational specifications, which allow for aggressive rail maintenance grinding, not only existing RCF initiations are removed but at the same time the conditions are set for the reappearance and further development of RCF cracking – at least for rails that are being loaded in the RCF-regime:

- on heat-treated premium pearlitic rails (tested in the version R370crHT/MHH) both by introducing a plastic deformation of the surface material toward the inside of the rail over the surface at the gauge side of the rail profile ('prestraining') and by generating large FIM deposits at the grooves, immediately resulting into large-scale crack initiation upon subsequent train operation;
- on standard carbon pearlitic rails (tested in the version R260Mn) by introducing plastic deformation of the gauge material toward the inside of the rail, coinciding with the plastic strain field as a result of plastic ratchetting under repetitive tangential wheel-rail contact stresses.

The difference in response between standard and heat-treated rail material with respect to the imprint of FIM portions under combined normal – tangential loading either in an elastic or a destructive mode can be further clarified from the constitutive properties. The heat treatment of the pearlite yields a grain refinement (which basically aims at delaying crack growth) and increases both the yield strength R_y (or $R_{p0.2}$) and the tensile strength R_m; however their ratio is not specified in the norm [1] and varies in practice. The ratio $\left(R_m - R_{p0.2}\right)/R_m$ can be taken as a measure to quantify the work hardening capacity in relation to the ultimate tensile strength; this value is about 46 percent for R260Mn versus 27 percent for R370crHT/MHH, whereas the tensile strength of the latter is roughly 41 percent higher as compared to the first (where average values are based on product certificates of both rail types). It follows from the previous that tensile strength is an important parameter with respect to RCF, but that the hardening capacity, which is not strictly prescribed by the norm, equally governs the life-cycle performance.

In the literature, the relationship between surface finishing techniques and RCF susceptibility has been addressed not in a rail-related but an industrial context, in a couple of dedicated studies and notably comparing grinding and hard turning techniques for hardened construction steel [7-10]. According to these studies, the hard turning technique is able to introduce compressive stresses, beneficial with respect to RCF, to a significantly greater depth in the subsurface as compared to grinding, which introduces normally compressive surface stresses, but with a steep gradient into the subsurface. The latter introduces high shear stresses parallel to the surface, and therefore a susceptibility to spalling, as argued in [13]. However, in the case of generation of a white layer, the surface residual stresses may become tensile (up to depths of 0.1 mm), favouring easy crack propagation. Although both surface finishing techniques may give rise to the generation of an – eventually stratified – WEL, thickness and hardness are different in both cases. In general, grinding tends to produce a much thicker WEL than turning. For both techniques, a white layer is found to drastically reduce the RCF life. Generally, RCF life of a component is found inversely proportional to the thickness of the white layer. Abusive grinding, introducing white layers and surface tensile stress, yields a reduction of the RCF life (start of surface spalling) with roughly a factor 9 as compared to gentle grinding with surface compressive residual stresses (Fig. 8 in reference [10]).

As has been mentioned in the introduction, the observed rail spalling defects grow relatively very fast with respect to conventional running band defects such as squats. In this context, a very significant difference in growth rates between ‘stud’ and ‘squat’ defects has been reported, with roughly 1 mm growth per 2.5 MT (megaton traffic load) for studs and flaking defects [3, 14] where, depending on other factors, between 50-100 MT is needed to grow a squat or other regular RCF defect on head-hardened rail [15, 16]. It is difficult to compare both defects in terms of growth rate in depth direction, taking into account that a spalling defects expands mostly horizontally in the subsurface whereas a squat defect also grows in depth. It can however be stated generally that spalling defects develop during megatons of cumulative loading, whereas squat cracks develop during tens of megatons; i.e. roughly a factor 10 slower. This factor is fully supported by the laboratory testing results from the literature in an industrial context discussed above. At the same time, the presence of severe subsurface residual (tensile) stress fields may also explain the striking geometry and location of the surface-breaking crack line of the spalling defects in Figs. 8 and 9, where this crack line delimits the periodic zone with the deepest grinding marks.

It is finally worth to consider in this context also the effect of third bodies in the wheel-rail interface. An important element in the composition of grinding stones (in grinding units of both manual and train-based equipment) is aluminium(III)oxide or aloxite Al_2O_3, which is used for its combined strength and hardness yielding excellent abrasive properties, and at the same time low costs. Different rail lubricants (friction modifiers), for different reasons also contain Al_2O_3 [17]. In the presence of repeated wheel slip (either full slip or microslip within the contact such as spin slip) this element may give rise to the development of white etching material on the surface of wheels and heat-treated rails. In the light of the findings of this work, the use of Al_2O_3 and similar compounds in lubricants should be considered in relation to RCF initiation on premium rails.

6. Conclusions

Spalling defects, over lengths up to hundreds of meters, on heat-treated pearlitic rails exhibit typical periodicity in geometry, in material properties such as hardness and the presence of a WEL, and in the position of crack initiation in the running band. This suggests a relationship between maintenance grinding on a regular basis and the initiation of RCF. In order to clarify the role of the 'initial conditions' of the rail service life in the RCF regime, effects of train-based maintenance grinding (as it is applied on the Dutch network and many other networks) have been investigated experimentally for two rail grades, one from the standard and one from the and heat-treated pearlitic rail category. The following conclusions can been drawn from this study:

1) on standard grades, friction-induced martensite (FIM), generated during grinding, delaminates during consecutive train operation. However, the applied grinding process

induces severe plastic top layer deformation which coincides with that induced by train operation. This yields ‘pre-fatigue’ of the rail.

2) On heat-treated grades, portions of FIM accumulate at groove edges during the grinding process. Under train operation, they are pressed into the deeper pearlitic matrix, in combination with severe plastic deformation as a result of tangential wheel-rail contact stresses. This yields extensive crack initiation, at the onset of the service life.
3) According to quantitative test results for industrial components reported in the literature, abusive grinding, which results into a white layer accompanied by harmful tensile residual stresses at the surface, yields a reduction with roughly a factor nine of the normal RCF life. This is in full accordance with observations on the growth of spalling defects on heat-treated rails, performing in the RCF regime, in the field, which develop within megatons of cumulative traffic loading. It is also in agreement with the difference in growth rate of roughly a factor ten between ‘stud’ and ‘squat’ defects reported in the literature.

In order to avoid spalling damage, at least operational grinding specifications for rails need to be reconsidered such that the formation of white etching layers, accompanied by harmful residual stress fields, are avoided, with special attention for heat-treated grades.

7. Acknowledgements

The specific grinding experiments described in this paper were initiated and carried out by Delft University of Technology in the framework of a more generic long-term study into rail degradation and the performance of cyclic grinding on the Dutch network, the latter for ProRail (Willem van Ginkel, Bob van Dijk). Ruud van Bezooijen (RailOK) organised the rail sample collection in the track and was in charge of the in-situ repair welding, both under critical time pressure.

References

[1] European Norm EN 13674-1, Railway applications - Track - Rail - Part 1: Vignole railway rails 46 kg/m and above (2011).

[2] S.L. Grassie, D.I. Fletcher, E.A. Gallardo Hernandez, P. Summers, Studs: a squat-type defect in rails, Proc. Inst. Mech. Eng. F: J. Rail and Rapid Transit, 226 (2012) 243-256.

[3] S.L. Grassie, Studs and squats: the evolving story, Proc. Int. Heavy Haul Conf. 2015, Perth, Australia, 21-24 June, 2015.

[4] M.C. Burstow, Whole life rail model application and development for RSSB – development of an RCF damage parameter, Tech. Rep. AEA Technology Rail, Derby, October 2008.

[5] V. Dikshit, P. Clayton, D. Christensen, Investigation of rolling contact fatigue in a head-hardened rail, Wear 144 (1991) 89-102.

[6] Y. Satoh, K. Iwafuchi, Effect of rail grinding on rolling contact fatigue in railway steel used in conventional line in Japan, Wear 265 (2008) 1342-1348.

[7] Y. Matsumoto, F. Hashimoto, G. Lahoti, Surface Integrity Generated by Precision Hard Turning, Annals CIRP 48 (1999) 59-62.

[8] D.W. Schwach, Y.B. Guo, A fundamental study on the impact of surface integrity by hard turning on rolling contact fatigue, Int. J. Fatigue 28 (2006) 1838-1844.

[9] F. Hashimoto, Y.B. Guo, A.W. Warren, Surface Integrity Difference between Hard Turned and Ground Surfaces and its Impact on Fatigue Life, Annals CIRP 55 (2006) 81-84.

[10] Y.B. Guo, A.W. Warren, F. Hashimoto, The basic relationships between residual stress, white layer, and fatigue life of hard turned and ground surfaces in rolling contact, CIRP J. Manufacturing Science and Technology 2 (2010) 129-134.

[11] M.J.M.M. Steenbergen, Squat formation and rolling contact fatigue in curved rail track, Eng. Fracture Mech. 143 (2015) 80-96.

[12] M.J.M.M. Steenbergen, R.P.B.J. Dollevoet, On the Mechanism of Squat Formation on Train Rails. Part I: Origination, Int. J. Fatigue 47 (2013) 361-372.

[13] M.J.M.M. Steenbergen, R.P.B.J. Dollevoet, On the Mechanism of Squat Formation on Train Rails. Part II: Growth, Int. J. Fatigue 47 (2013) 373-381.

[14] F. Fau, H. Smith, S. Fretwell-Smith, L. Deng, Effect of grinding quality, lubrication quality and rail hardness on flaking defect initiation on high rails, Proc. 10th Int. Conf. Contact Mech. Wear Rail/Wheel Systems CM2015, Colorado, USA, 30 Aug. - 3 Sept., 2015.

[15] R. Heyder, M. Brehmer, Empirical studies of head check propagation, Proc. 9th Int. Conf. Contact Mech. Wear Rail/Wheel Systems CM2012, Chengdu, China, 27-30 Aug., 2012.

[16] K. Kondo, K. Yoroizaka, Y. Sato, Cause, increase, diagnosis, countermeasures and elimination of Shinkansen shelling, Wear 191 (1996) 199–203.

[17] M. Oomen (Twente University, Surface Technology & Tribology), Personal communication with the author, 2015.